Study on Interaction of Coomassie Brilliant Blue G-250 with Bovine Serum Albumin by Multispectroscopic

Mingjun Yang[1] · Dongxiang Shi[1] · Yonggang Wang[1] · Abdol Ghaffar Ebadi[2] · Mohsen Toughani[3]

Abstract

Aim of present study was to investigate the interaction of coomassie brilliant blue G-250 (CBBG-250) with bovine serum albumin (BSA) by the multispectroscopic methods. Fluorescence-data showed that the complex of BSA-CBBG-250 forming made the intrinsic fluorescence quenching of BSA by CBBG-250 interaction. BSA also could interact with CBBG-250 and the CBBG-BSA complexes formed in a molar ratio of 1:1. UV–Vis results displayed that the apparent binding (association) constant K_a of CBBG-250 with BSA was 5.03×10^4 (298 K), 3.04×10^4 (303 K), 2.84×10^4 (308 K) and 1.99×10^4 (313 K) L mol^{-1} at different temperatures, respectively. The enthalpy change ($\triangle$H) and entropy change ($\triangle$S) were respectively calculated to be -45.32 kJ mol^{-1} and -139.18 J mol^{-1} K^{-1}, indicating that the hydrogen bonds and *Van der Waals* forces played dominant roles in the interaction. The results showed that the diphenylamine structure and amino acid residues in the Coomassie Brilliant Blue G-250 had a strong Van der Waals force. The phenyl sulphonic acid group undergoes electrostatic interactions and hydrogen bond interactions with basic amino acids; the compound Coomassie Brilliant Blue G-250 can form a stable complex with BSA.

Keywords Bovine serum albumin · Coomassie brilliant blue G-250 · Interaction · Spectrum

Introduction

Coomassie brilliant blue G-250 (CBBG-250), known as a chemical dye, has a molecular formula of $C_{47}H_{48}N_3O_7S_2Na$ whose structure is shown in Fig. 1. Bradford (1976) first reported the Bradford assay that Coomassie Brilliant Blue G-250 could bind to Bovine Serum Albumin to form a protein–dye complex and had the linear correlation at a wavelength of 595 nm. This method provided a general and quantitative way to measure protein. Considering this method has attractive features including high sensitivity and specificity, simple operating, less interference factors, it has been commonly used in biochemistry analysis. Currently, the research on CBBG-250 and biological macromolecular protein mainly focused on two aspects: (I) study of discoloration mechanism Coomassie brilliant blue G-250 (Guo and Jiang 1996; Macart and Gerbaut 1982; Compton and Jones 1985; Cao et al. 2002, 2008) and determination process improvement (Schaffner and Weissmann 1973; Spector et al. 1978; Duhamel et al. 1981; Löffler and Kunze 1989; LãPez et al. 1993; Chen et al. 2009; Wang et al. 2013, 2017; Liang et al. 2018; Yang et al. 2020; Ren et al. 2018). In contrast to above study, little reports were known about the interaction mechanism between CBBG-250 and protein. In previous studies, authors separately measured the absorbance values of BSA, bovine hemoglobin, pepsin, trypsin, Type I and II collagen at the same molarity by using the Bradford method, the results showed that absorbance values of CBBG-250 response to different proteins exist significant differences (Wang et al. 2013). Thus, we considered that the difference of protein composition and structure exhibited the different interaction way with CBBG-250.

Spectroscopy and Molecular modeling techniques are primary ways to research the interaction between small molecule compounds and macromolecules (Cao and Yufen 2004; Li et al. 2006, 2009). As early as 1894, the molecular docking method was first proposed by scientists at the molecular

✉ Yonggang Wang
  wangyg@lut.cn

1   School of Life Science and Engineering, Lanzhou University of Technology, Lanzhou 730050, China

2   Department of Agriculture, Jouybar Branch, Islamic Azad University, Jouybar, Iran

3   Department of Fishery, Babol Branch, Islamic Azad University, Babol, Iran
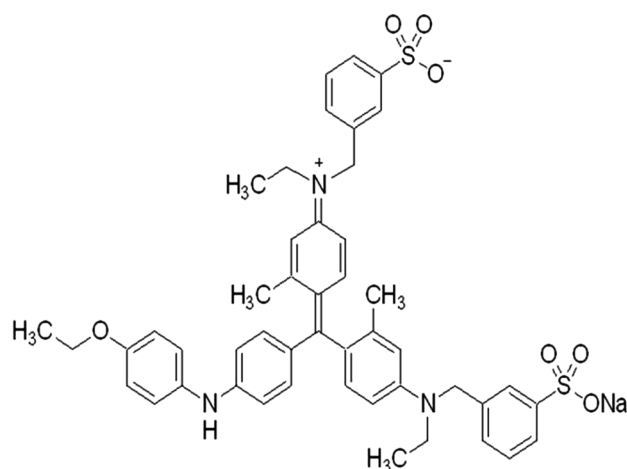
Fig. 1 Structures of CBBG-250

level to study chemical problems in biological systems. E. Fisher used the metaphor of a yoke and a key to describe the specific binding of an enzyme to a substrate, called recognition. At the same time, Langley's theory of receptors suggested that most drugs can bind to specific molecules on the cell membrane or inside cells. These specific molecules were called receptors. Therefore, the concept of acceptors in receptor theory was basically the same as that in molecular docking, which given a theoretical foundation for molecular docking methods. The high-throughput virtual screening technology (parallelized molecular docking method) had a large amount of screening, and it can complete testing of databases containing hundreds of thousands or even millions of compounds per day. In general, virtual screening was more efficient than empirical screening. Molecular docking techniques have become complementary to high-throughput screening to find lead compounds (Morris et al. 2008; Duan et al. 2009; Falchi et al. 2014; Shin and Kihara 2018; Pinzi and Rastelli 2019). In this study, the binding constants and the thermodynamic parameters between CBBG-250 and BSA were measured using fluorescence spectroscopy and ultraviolet spectroscopy, the changes of functional groups also were analyzed before and after intermolecular reaction by fourier transform infrared spectroscopy and circular dichroism spectrum, which were of great significance to explore the mechanisms of the interaction between CBBG-250 and BSA.

Materials and Methods

Apparatus and Reagents

Apparatus: Ultraviolet–Vis spectrophotometer (Cary 50, Varian, USA); Fluorescence spectrophotometer (RF-5301-PC, Shimadzu, Japan); Fourier Transform Infrared Spectrometry (FTIR-850, Nicole, USA); Circular dichroism (Jasco-20c, Shimadzu); Digital constant temperature water bath (HH-S, China); Electronic balance (AB104-N, mettler); pH Meter (PXSJ-226, Rex Electric Chemical, Shanghai, China).

Reagents: Coomassie brilliant blue G-250 (CBBG-250) was purchased from Shanghai solarbio Bioscience & Technology Company. Bovine serum albumin (BSA) was purchased from Roche Company. Absolute alcohol, 85% phosphoric acid and other reagents used were of analytical reagent grade. Distilled water was used throughout the experiment.

Preparation of the Reagents

0.1 mg/mL BSA solution preparation: 10 mg BSA were weighed on an electronic balance, dissolved and diluted with ultrapure water to give a final volume of 100 mL; 3.5 mg/100 mL CBBG-250: weigh accurately 3.5 mg CBBG-250, dissolved fully in 5 mL 95% ethanol, then add 10 mL 85% phosphoric acid, add ultrapure water to bring the volume up to 100 mL.

Fluorescence Spectra Measurements

Accurately take 1.0 ml BSA standard solution (0.1 mg/mL) to 10 mL colorimetric tube, 5 mL of different concentrations CBBG-250 solution and 4.0 mL ultrapure water were added, respectively, and then the mixture incubate for 10 min at 303, 308 and 313 K. Fluorescence spectra were recorded on a Spectrophotometer with the excitation wavelength of 280 nm, slit widths of 5 nm for both excitation and emission bandwidths. When the scanning interval of excitation and emission wavelength was fixed at 15 and 60 nm, respectively. Synchronous fluorescence spectroscopy between BSA and CBBG-250 were recorded over a wavelength range of 300–500 nm.

UV–Vis Spectrum Measurements

Under the temperature of 298 K, 303 K, 308 K and 313 K to analyze the UV–Vis absorption at 200–800 nm about the interaction of known concentrations of BSA and CBBG-250 solution of different concentrations which can be used to explore the largest absorption peak and measure the light absorption value in the maximum absorption peak and draw the corresponding curve of thermodynamics.

Fourier Transforms Infrared Spectrometry

Take a small amount of 0.1 mg/mL BSA, 3.5 mg/100 mL CBBG-250 solution respectively and mix well coating, analysis the functional groups correlated with the presence of itself, the different functional groups between two materials after reaction was recorded in the featured region of 4000–400 cm^{-1}, with 4 cm^{-1} resolutions at room temperature.

Circular Dichroism (CD) Measurements

Accurately take 5.0 mL CBBG-250 solution in 10 mL colorimetric tube, 1.0 mL BSA standard solution and 4 mL distilled water were added to a final volume, the samples were incubated for 10 min. the CD spectra of CBBG-250 in the absence and presence of BSA were recorded at a wavelength range of 200–280 nm with three scans times. The change of the α-helical contents in BSA was analyzed according to the following equation (Lee et al. 2012).

$$\alpha = \frac{-[\theta]_{208} - 4000}{33,000 - 4000} \times 100\%$$

Molecular Docking

The mechanism of Coomassie Brilliant Blue G250 and bovine serum albumin BSA (PDB ID: 4F5S) was studied at the molecular level using the molecular docking software Autodock vina 1.1.2. Firstly, the active sites of bovine serum albumin were found by bond energy analysis, and the possible conformation was obtained through virtual docking. With the affinity as the evaluation criterion, the highest affinity was found, the best conformation was docked, and their connection groups and interactions were determined.

Results and Discussion

The Florescence Spectrum of Interaction Between CBBG-250 and BSA

The Fluorescence Quenching Spectrum and Synchronous Fluorescence Spectrum for BSA and CBBG-250

BSA, a kind of endogenous fluorescent substances, includes three phenyl-structure amino acid residues with tryptophan, tyrosine and phenylalanine which can be capable of emitting a certain intensity of endogenous fluorescent (Shahabadi et al. 2011). Among them, tryptophan residue is the high one. The excitation wavelength was

set at 280 nm and the concentration of CBBG-250 was changed by degrees, then we scanned the fluorescence spectrum (Fig. 2). This result shows that the emission wavelength of BSA is 342 nm and its fluorescence intensity quenches with increasing concentration of CBBG-250, suggesting that interaction between CBBG-250 and BSA occurred as well as increased the polarity of Amino acid microenvironment.

In order to gather some insights into the interaction of CBBG-250 with BSA, to understand the conformational change of BSA, we performed the synchronous fluorescence spectra analysis. When the wavelength interval (Δλ) between excitation and emission wavelength is 15 or 60 nm from 300 to 500 nm, the synchronous fluorescence spectra offer the characteristics of tyrosine residues and tryptophan residues of BSA. The maximum emission wavelength of above two amino acids was relevant to the polarity of their microenvironment. A blue shift in their maximum emission wavelength with the increase of the hydrophobicity of its environment was observed, on the other hand, the red shift (Lloyd 1971). Figure 3a and b respectively shows the synchronous fluorescence spectra condition (Δλ = 15 nm and Δλ = 60 nm) of BSA interact with CBBG-250. As seen from above Figure, when Δλ = 15 nm, with the increase of concentration of CBBG-250, no obvious wavelength shift was observed at the maximum emission wavelength (312 nm), in contrast, when Δλ = 60 nm, synchronous fluorescence spectrum of the maximum emission wavelength has a remarkable red shift (342 nm–350 nm). The results indicated that the hydrophobicity in the environment around the tryptophan residues of BSA was decreased with the join of CBBG-250.
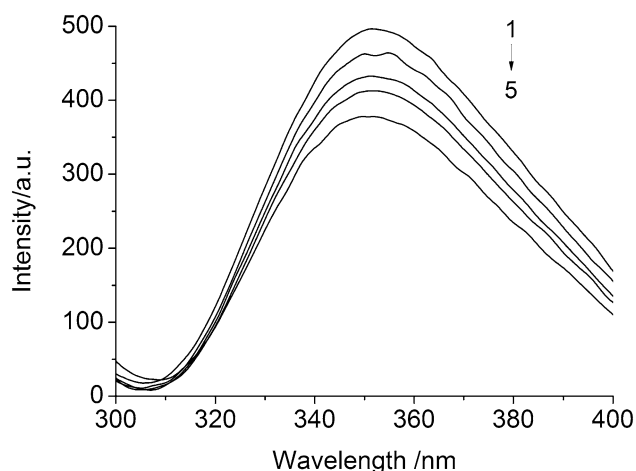
Fig. 2 Fluorescence emission spectra of BSA with different concentration of CBBG-250. c(BSA) = 1.49 μmol L^{-1}, λex = 280 nm, T = 303 K, (1→5) notes the concentration of CBBG-250 was 0, 35.13, 40.98, 46.8, 52.69 μmol L^{-1}, respectively
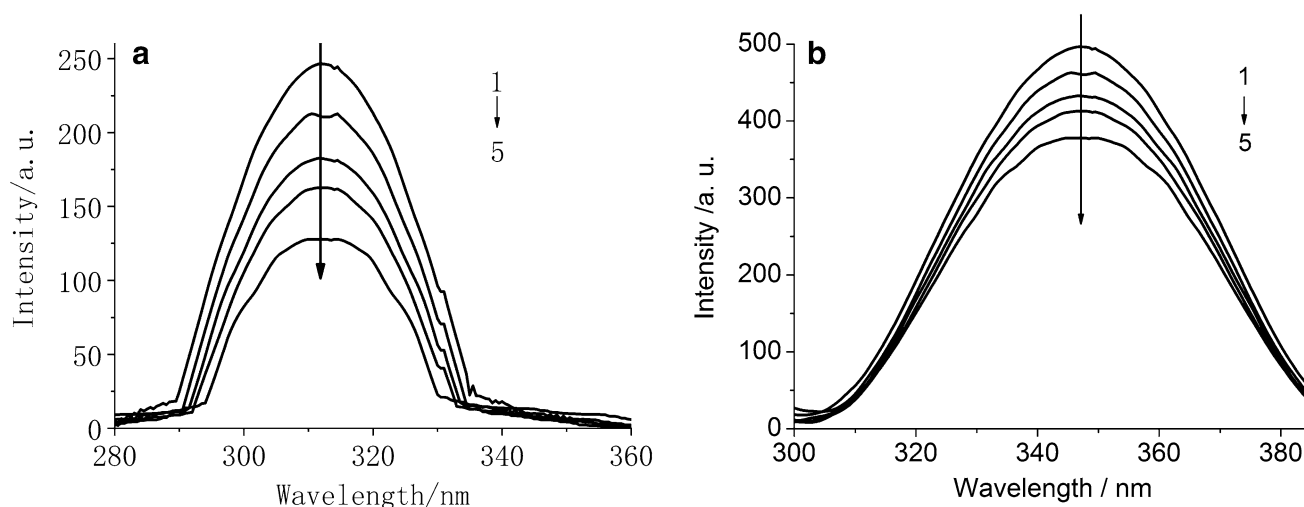
Fig. 3 Synchronous fluorescence spectra of BSA in the absence and presence of CBBG-250. **a** $\Delta\lambda = 15$ nm; **b** $\Delta\lambda = 60$ nm. T = 303 K, c(BSA) = 1.49 μmol L^{-1}, the concentration of CBBG-250 (1→5): 0, 35.13, 40.98, 46.8, 52.69 μmol L^{-1}
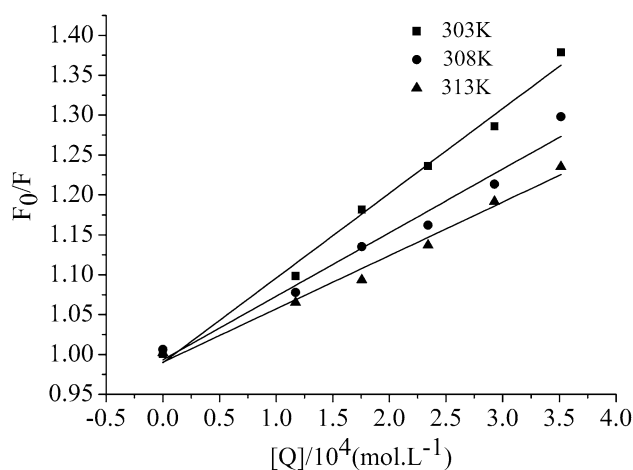
The mechanism of fluorescence quenching

Fluorescence quenching refers to a physical or chemical process between the fluorescent substance and the solute molecules, lead to the changes of fluorescence intensity or related excitation peak position. It can be classified as dynamic quenching or static quenching. For dynamic quenching, the number of ion effective collision to increase with increasing temperature, electron transfer starts intensify, the bimolecular quenching constants are also increase with increasing temperature. In contrast, in static quenching process, increased temperature is likely to result in decreased stability of complexes, make the bimolecular quenching constants decrease. In order to confirm the quenching mechanism of BSA and CBBG-250, we analyzed the fluorescence quenching of BSA under different temperature according to the well-known Stern–Volmer equation (Shahabadi et al. 2011):

$$\frac{F_0}{F} = 1 + K_q\tau 0[Q] = Ksv[Q]$$

In the above formula: F_0 and F represent the steady-state fluorescence intensities in the absence and presence of quencher (CBBG-250) respectively; K_q is the quenching rate constant of biomolecular, it reflects the molecules collide with each other and mutual diffusion affect the fluorescence lifetime of the biopolymer; τ_0 is the average lifetime of biomolecular without the quencher and its value is 10^{-8} s; [Q] is the concentration of quencher; K_{sv} is the Stern–Volmer quenching constant, which describes the biological macromolecules and fluorescence quencher diffused and collided with each other reached the concentration–response relationship to achieve dynamic balance, Ksv = Kqτ_0 (Ware 1962).

In our experiments, we studied fluorescence spectrum of the interaction between CBBG-250 and BSA at 303 K, 308 K, 313 K, Calibration curve of $\frac{F_0}{F}$ shows the linearity against the corresponding CBBG-250 concentration, the results are shown in Fig. 4. Stern–Volmer curves are in good linear relationship at various temperatures, with the temperature increases, the slope of Stern–Volmer plot decrease, values for K_q were 1.061×10^{11} L moL^{-1} s^{-1} (303 K), 0.79686×10^{11} (308 K) and 0.66881×10^{11} (313 K). Moreover, the minimum K_q value is much greater than the maximum diffusion collision quenching rate constant (2.0×10^{10} M^{-1} s^{-1}) of a variety of quenchers with biopolymer. The quenching constant is decreasing with increasing temperature, and the results obtained from the fluorescence

Fig. 4 Stern–Volmer curves of fluorescence quenching of BSA by CBBG-250 at different temperatures
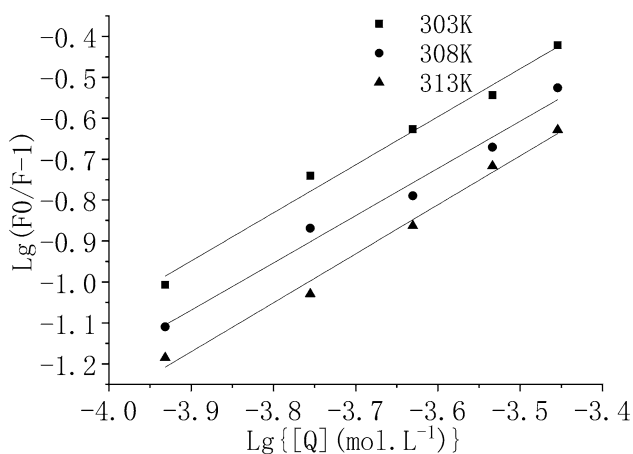
spectroscopy indicated that an interaction occurred between CBBG-250 and BSA through a static quenching type.

The Binding Constant (Ka) and Number of Binding Sites (n)

The result of fluorescence spectrum analysis shows that interaction between CBBG-250 and BSA through a static quenching type. So according to the following equation (Li et al. 2009):

$$\lg \frac{F_0 - F}{F} = \lg K + n\log[Q].$$

Figure 5 shows the linearity in the plot $\lg \frac{F_o - F}{F}$ against $\lg[Q]$. The CBBG-250 and BSA binding constant (K_a) and number of binding sites (n) was calculated through the slope and intercept of the straight line. The corresponding values of K_a and n are presented in Table 1. The table data showed that CBBG-250 and BSA have strong interaction with the binding constant of 10^3. In addition, the values of binding constant were reduced by the temperature increasing, suggesting the combination capabilities of CBBG-250 with BSA were greatly influenced by temperature.

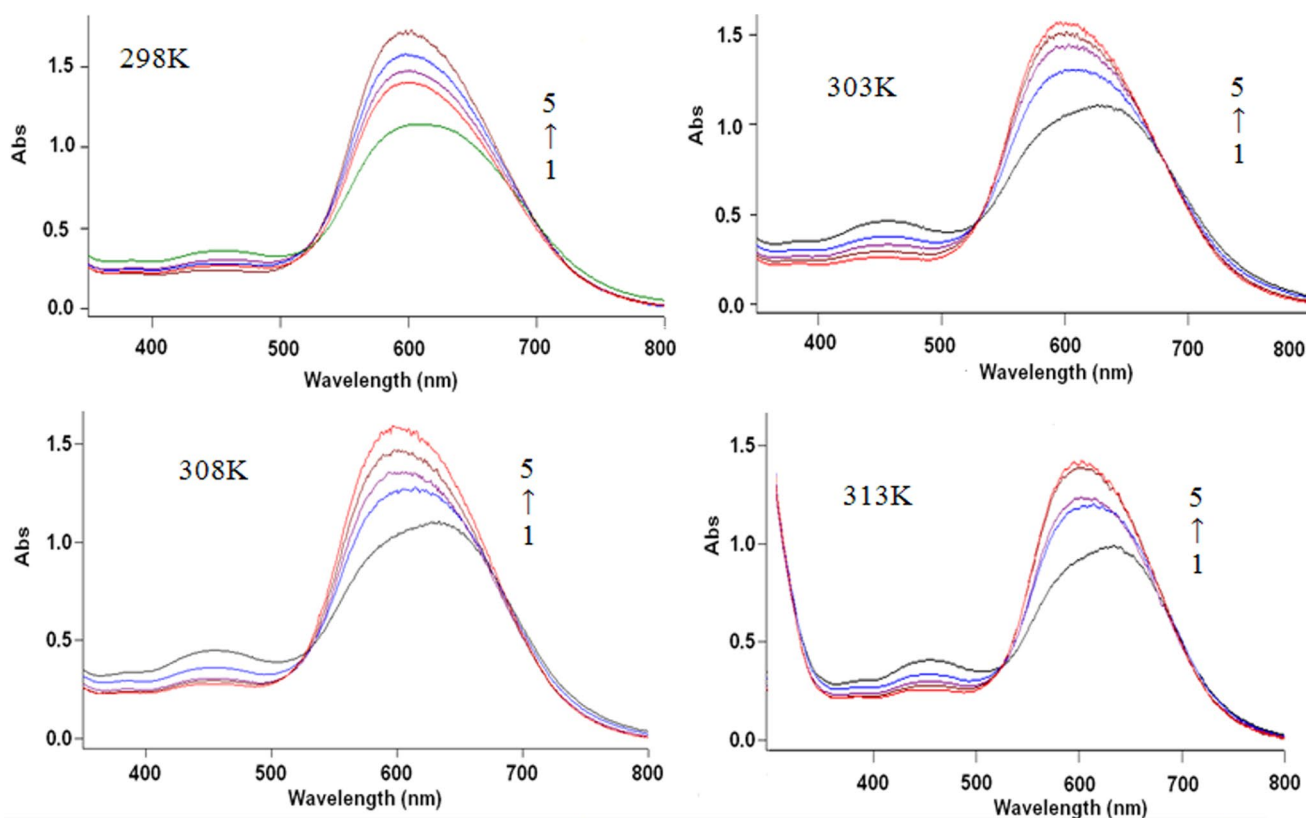**Fig. 5** Double-log plot of CBBG-250 quenching effect on BSA fluorescence at different temperatures

Identification of Interaction Force Between CBBG-250 and BSA

The acting forces between small molecules and biological macromolecules may include hydrophobic force, electrostatic interactions, *Van der Waals* interactions, hydrogen bonds. They were belongs to the weak interaction between the molecules. The negative value of ΔG revealed that the interaction process was spontaneous. The relative value of the entropy change (ΔS) and enthalpy change (ΔH) before and after the reaction can determine the acting forces between small molecules and proteins: ΔH > 0, ΔS > 0 exhibited the binding style of interaction force between two component was hydrophobic force; ΔS < 0, ΔH < 0 implied the binding style of interaction force between two component was the *Van der Waals* force and hydrogen bonds; ΔH < 0, ΔS > 0 displayed the binding style of interaction force between two component was electrostatic interactions (Ross and Subramanian, 1981; Wu et al. 2019). Therefore, according to the thermodynamic functions: $\Delta G = -RT\ln K$ and $\ln \frac{K2}{K1} = \left(\frac{1}{T1} - \frac{1}{T2}\right) \frac{\Delta H}{R}$, $\Delta G = \Delta H - T\Delta S$, Table 1 showed thermodynamic parameters of CBBG-BSA reaction process, the value ΔH < 0, Δ S < 0 indicated that the binding style of interaction force between CBBG-250 and BSA was mainly for hydrogen bonding and *Van der Waals* force. Hence, the binding process was always spontaneous It can be concluded that in the condition of different temperature, the interaction process between CBBG-250 and BSA gradually tend to be stable. ΔH < 0 indicated that the reaction was a exothermic process, the spontaneous process between CBBG-250 and BSA molecular was mainly driven by positive entropic changes.

UV–Vis Spectrum Measurements Between CBBG-250 and BSA

UV–Vis Spectrum of Interaction Between CBBG-250 and BSA

The combination effects between a fixed concentration CBBG-250 and various concentration BSA under the temperature of 298 K, 303 K, 308 K, 313 K were analyzed using a UV–Vis spectrum with a wavelength of 200–280 nm. From the Fig. 6, the characteristic absorption peak of the

Table 1 Thermodynamic parameters of CBBG-BSA reaction process

T/K	K/(mol/L)$^{-1}$	n	r	G/(kJ mol^{-1})	ΔH/(kJ mol^{-1})	ΔS/(J K^{-1}·mol^{-1})
303 K	4251.087	1.1736	0.9903	− 2.53	− 4.38	− 6.1598
308 K	3118.172	1.1959	0.9965	− 2.48		
313 K	2675.469	1.1528	0.9958	− 2.47		

Fig. 6 UV–Vis spectra of CBBG-250 with different concentration of BSA. c(CBBG-250) = 0.05 mg/mL, (1→5) shows the concentration of BSA is 0.02, 0.04, 0.06, 0.08, 0.1 mg/mL, respectively

combination of CBBG-250 and BSA was 595 nm, the absorption value also increased with the increase of concentration of BSA, and exhibited a well linear relationship. In addition, and when the temperature is 313 K, the linear relationship is poor under the same condition and the increase of absorption value slowed down. It suggested that the temperature had an effect on the combination between CBBG-250 and BSA.

Binding Constant (Ka) and CBBG-250 Type with the Active Force of BSA

The reaction equation between CBBG-250 and BSA could be expressed as n CBBG-250 + BSA = BSA-CBBG-250n, In the Fluorescence Spectroscopy research, the number of binding site (n) of the interaction of CBBG-250 with BSA was 1, so:

$$K = \frac{BSA - CBBG - 250n}{[CBBG - 250]n[BSA]} \quad (1)$$

By Eq. (1),

$$[BSA]_0 = [BSA] + [BSA - CBBG - 250 \cdot n]$$
$$= [BSA] + K \cdot [BSA][CBBG - 250] \cdot n \quad (2)$$

$$[CBBG - 250]_0 = [CBBG - 250] + [BSA - CBBG - 250 \cdot n]$$
$$= [CBBG - 250] + K \cdot [BSA][CBBG - 250] \cdot n \quad (3)$$

In the formula, $[BSA]_0$ and $[CBBG-250]_0$, respectively, for the initial concentration of BSA and CBBG-250. We suppose $[BSA]_0 \geq [CBBG-250]_0$ that can infer $[BSA] \approx [BSA]_0$, by Eq. (3),

$$[CBBG - 250]n = \frac{[CBBG - 250]_0}{1 + K[BSA]_0} \quad (4)$$

Because $[BSA]_0 \geq [CBBG-250]_0$ and the absorbance ratio A is in direct proportion to the [BSA-CBBG-250n] that comply with Beer-Lambert's Law, that is

$$A = \varepsilon \cdot [BSA - CBBG - 250n] \cdot L \quad (5)$$

In the equation, the ε is molar absorption coefficient and the L (cm) is thickness of the pool suction light.

According to the formula (1), the Eq. (5) could be converted into (6):

$$A = \varepsilon \cdot K \cdot [BSA] [CBBG \text{-} 250] \cdot n \qquad (6)$$

The formula (6) also can be expressed as (7)

$$A = \varepsilon K \cdot \frac{[CBBG \text{-} 250]_0}{1 + K \cdot [BSA]_0}[BSA]_0 \qquad (7)$$

Because of $[BSA] \approx [BSA]_0$, the Eq. (7) is converted to (8)

$$\frac{[CBBG \text{-} 250]_0}{A} = \frac{1}{K\varepsilon} \cdot \frac{1}{[BSA]_0} + \frac{1}{\varepsilon} \qquad (8)$$

The formula (8) is simplified to be (9)

$$\frac{1}{A} = \frac{1}{K\varepsilon \cdot [CBBG \text{-} 250]_0} \cdot \frac{1}{[BSA]_0} + \frac{1}{\varepsilon \cdot [CBBG \text{-} 250]_0} \qquad (9)$$

Mapping from $\frac{1}{A}$ and $\frac{1}{[BSA]_0}$, we can obtain K_a and ε from the slope and intercept. At the same time, $\ln K = \frac{H}{RT} + \frac{S}{R}$. We can work out the $\triangle H$ and $\triangle S$ from slope and intercept in the working curve between $\ln K$ and $\frac{1}{T}$.

In this study, the UV–Vis spectroscopy spectra of CBBG-250 with BSA at the temperature of 303 K, 308 K and 313 K were investigated at a wavelength of A_{595} nm. At different temperature, the working curve between 1/A and

$1/[BSA]_0$ could be drawn and the correlation coefficient (r) were obtained as shown in Fig. 7. The curves at different temperature all showed a good linear relationship with the increase of concentration of BSA. But, the absorbance value and slope decreased with the increase of temperature. The forming constants (k) was calculated respectively by the slope and intercept of the combination of different temperature (Table 2). From the Table 2, we can see the k value decreased with the increase of temperature that suggested temperature changes greatly influenced the role of CBBG-250 with BSA. In the woring curve between ln k and 1/T (Fig. 8), we can infer that $\triangle G < 0$ and $\triangle G$ increases with the increase of temperature. Hence, it can be inferred that the reaction of different concentration BSA and CBBG-250 at different temperature was a spontaneous process and this process gradually tend to be stable. and $\triangle H < 0$ shows that the reaction was exothermic process. The reaction of BSA and CBBG-250 existed hydrogen bonds and Van der Waals force in the process.

Ultraviolet Absorption Spectrometry

Add different concentrations of CBBG-250 into the certain concentration of BSA solution in turn, the ultraviolet–visible absorption spectrum of scanning was determined in the range 200 nm-800 nm. The result is shown in Fig. 9,
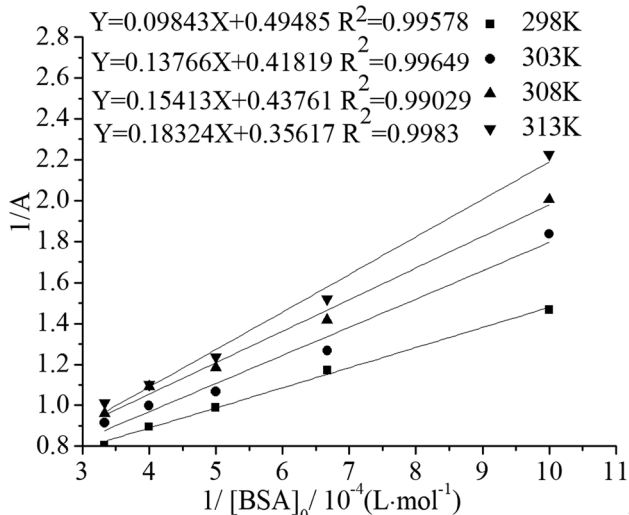

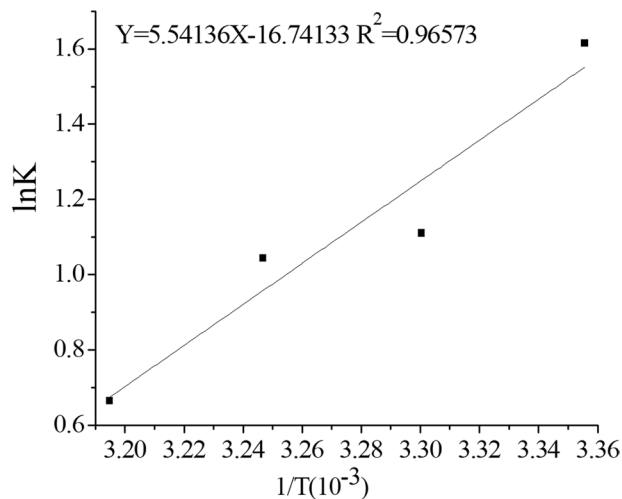**Fig. 7** Curves of $1/[BSA]_0$ and 1/A at different temperatures

Y=0.09843X+0.49485 R^2=0.99578 ■ 298K
Y=0.13766X+0.41819 R^2=0.99649 ● 303K
Y=0.15413X+0.43761 R^2=0.99029 ▲ 308K
Y=0.18324X+0.35617 R^2=0.9983 ▼ 313K

Fig. 8 Curves of 1/T and lnK at different temperature

Y=5.54136X-16.74133 R^2=0.96573

| Table 2 Thermodynamic parameters of BSA-CBBG-250 reaction process	T/K	K/(mol/L)$^{-1}$	r	$\triangle G$/(kJ· mol^{-1})	$\triangle H$/(kJ· mol^{-1})	$\triangle S$/(J·K^{-1}·mol^{-1})
	298 K	5.03×10^4	0.9983	− 4.0021	− 45.3229	− 139.1847
	303 K	3.04×10^4	0.9903	− 2.7984		
	308 K	2.84×10^4	0.9965	− 2.6726		
	313 K	1.99×10^4	0.9958	− 1.7963		
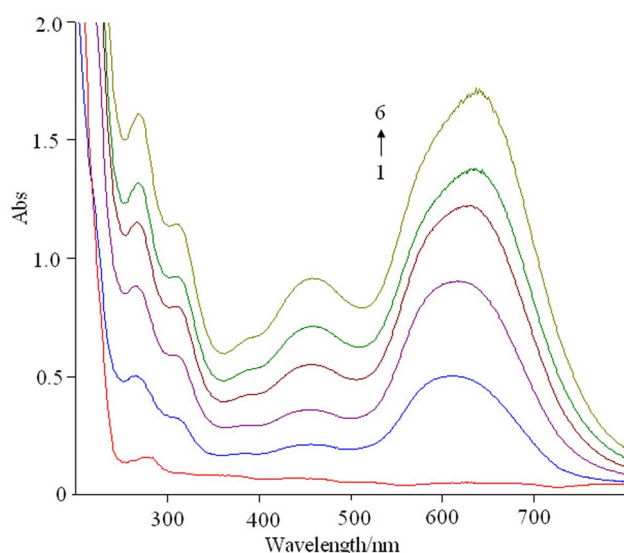
Fig. 9 UV–Vis absorption spectra of BSA in the presence of various concentrations of CBBG-250. $c(BSA) = 1.49$ μmol·L^{-1}, T = 303 K, $(1 \rightarrow 5)$ notes the concentration of CBBG-250 is 0, 35.13, 40.98, 46.8, 52.69, 58.34 μmol·L^{-1}, respectively

The BSA had two absorption spectra with the position peaks at 203 nm and 274 nm (the reports in the literature is 220 nm and 278 nm) (Duan et al. 2009), the absorbance with a position peak at 274 nm was mainly due to these bases undergone n to π* and π to π* transitions from aromatic side chains of tryptophan, tyrosine in BSA molecules. While the absorption peaks for BSA at 203 nm in an UV–Vis spectrum was mainly due to the bases undergo n to π* transitions from C=O in the polypeptide backbone, which was also associated to the α-helix content in BSA (Shahabadi et al. 2011). The hyperchromic effect was discovered with increasing protein concentration. The conformation of BSA has also changed, inducing the extension of peptide bond in the BSA molecules, which makes the aromatic heterocyclic of chromophore (like tryptophan and tyrosine) expose, leading to the increasing of absorbance. Meanwhile, the characteristic absorption peak of CBBG-250 solution appeared at 465 nm with the increase of CBBG-250 solution, and a characteristic peak of the complex structure of BSA–CBBG-250 also exhibited in the UV–Vis region at 600 nm. Together, these results further showed that an interaction occurred between CBBG-250 and BSA and it was a saturation reaction.

Fourier Transforms Infrared Spectrometry

Fourier transform infrared spectroscopy is often used to study hydrogen bonding interactions. In order to gather some insights into the changes in the secondary and functional groups of BSA, a detailed analysis of the every components
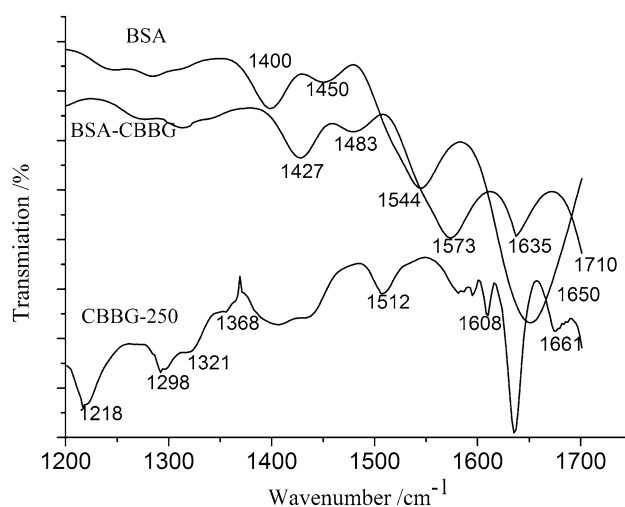
Fig. 10 FT-IR spectra of the interaction BSA and CBBG-250

of BSA in the absence and presence of CBBG-250 was carried out by Fourier transform infrared spectroscopy. The amide bands of the proteins in infrared area, amide I ranging from 1600 to 1700 cm^{-1} (mainly C=O) and amide II 1548 cm^{-1} (mainly C–N and N–H) have been widely used as typical properties. In Fig. 10, the position peak of BSA without significant change with the addition of CBBG-250, but the amide I band was blue-shifted (from 1650 to 1710 cm^{-1}), the structure of α-helix in BSA (of 1650–1658 cm^{-1}) and β-sheet in BSA (the band characteristics 1620–1640 cm^{-1}, 1675 cm^{-1}) has been changed. Moreover, an decrease of the structure of α-helix was observed (Byler et al. 1986; Zhang et al. 2012).

One possible reason was that the formation of the complex of BSA–CBBG-250 induced amino, carboxyl hydrogen in the peptide to occur large rearrangements. Sulfonic acid group, amino group, hydroxy benzene in CBBG-250 molecules can not only could react or form hydrogen bonding with amino group, hydroxyl group and carboxyl group in the protein side chain, but also can form a hydrogen bond structure with the peptide bond to change the stretching vibration of –C=O, C–N, which can lead to plane bending of –NH. As a result, the peak position of amide band changed, so as protein secondary structure also was changed (SUN 2013).

Circular Dichroism

The typical structural features of BSA was that α-helix have negative cotton effects at 212 nm and 215 nm, β-sheet conformation with a characteristic negative peak was at about 215 nm, one positive peak of the random coil at 220 nm appeared (Demchenko 1988).

The CD spectra of BSA and CBBG-250-BSA complex were shown in Fig. 11. As can be seen from Fig. 11, the
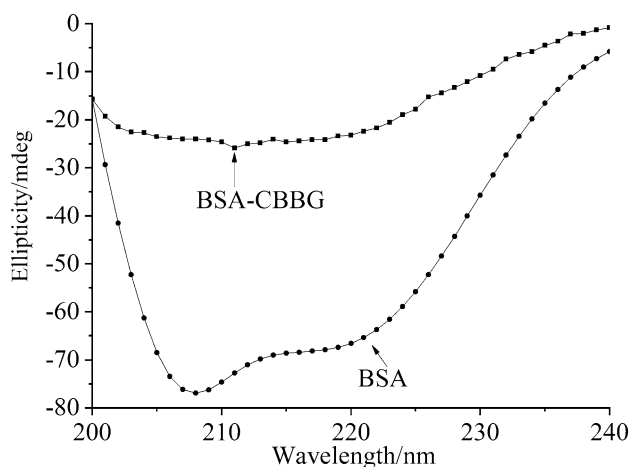
Table 3 Molecular docking results

Conformation	Affinity (kcal/mol)
1	− 8.1
2	− 8.0
3	− 7.6
4	− 7.5
5	− 7.3
6	− 7.1
7	− 7.0
8	− 6.9
9	− 6.8

Fig. 12 CBBG-250 docked to the active pocket of BSA
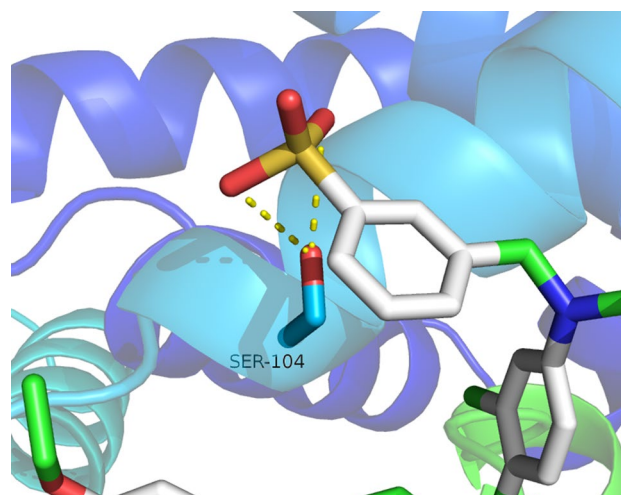

Fig. 13 Hydrogen bonding between CBBG-250 and amino acid SER104

CD spectrum of BSA exhibited two negative bands in the ultraviolet region at 209 and 222 nm, which was a characteristic of α-helical structure of protein. The binding of BSA to CBBG-250 caused no obvious change about the shape of the CD spectrum and peak position. Meanwhile the calculated results exhibit an decline of from 42.15 to 1.27%, most of the α-helical structure become to β-sheet. The results revealed that the secondary structure of BSA had been changed due to the binding of CBBG-250 to BSA. The reason may be that CBBG-250 interacted with the amino acid residues, which from the alpha helix by hydrophobic force and hydrogen bond, destroyed the alpha helix structure in BSA, thus resulting in a decline in alpha helix content.

Molecular Docking Results

In order to elucidate its mechanism of action from the molecular level, we docked Coomassie Brilliant Blue G-250 into the active pocket of BSA. The docking results were shown in Table 3, and 9 kinds of conformations were generated. We selected the conformation 1 with the highest affinity for study, and the results were shown in Fig. 12.

It can be seen from Fig. 12 that the diphenylamine structure in Coomassie Brilliant Blue G-250 molecule can strongly interact with amino acid residues GLN203, LYS204, ARG196, GLU464, ASP108, LYS465, LYS106 and TRP147. The phenyl sulfonic acid group on one side of the CBBG-250 molecule extended toward the basic amino acid HIS105, undergone electrostatic interactions, and simultaneously formed a double hydrogen bond with
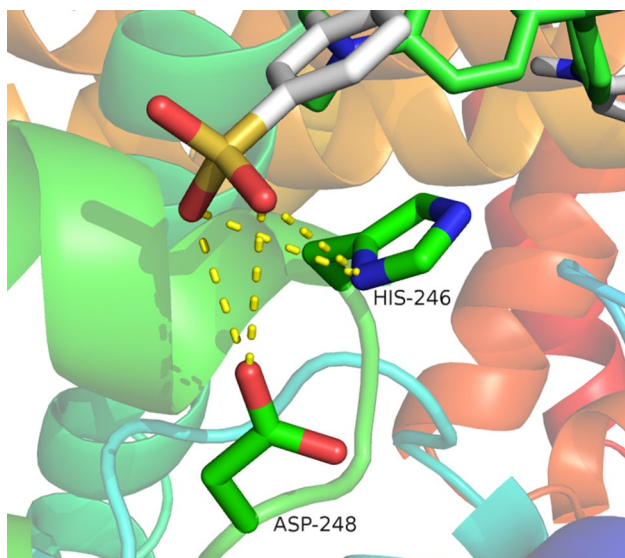
Fig. 14 Hydrogen bonding between CBBG-250 and amino acids HIS246 and ASP248

the amino acid residue SER104 (Fig. 13). The other side of the phenyl sulfonate structure formed electrostatic interactions with the basic amino acids LYS242 and HIS246. More importantly, its sulfonic acid structure can form a tetrahydrogen bond with amino acid residues HIS246 and ASP248 (Fig. 14). Due to the stable mode of action, the compound Coomassie Brilliant Blue G-250 can form a stable complex with BSA.

Conclusion

In this study, new evidences of binding of BSA to CBBG-250 were provided by fluorescence spectroscopy, circular dichroism (CD), Fourier transform infrared (FT-IR), and molecular docking. The results indicated that the binding of CBBG-250 to BSA interacted via static quenching, and that their binding changed the secondary structure of BSA. A stable complex of between CBBG-250 and the amino acid residue of BSA formed through hydrogen bonding, Van der Waals force and hydrophobic interaction, and the reaction is a saturated reaction. During this reaction, their binding ability was affected by heat-induced changes.

Compliance with Ethical Standards

Conflict of interest Authors have no conflict of interest.

References

Bradford M (1976) A rapid method for the quantification of microgram quantities of protein utilizing the principle of protein-dye binding. Anal Biochem 72(s1–2):248–254. https://doi.org/10.1016/0003-2697(76)90527-3

Byler DM, Brouillette JN, Susi H (1986) Quantitative studies of protein structure by FTIR spectra deconvolution and curve-fitting. Spectroscopy 3:29–32

Cao S, Yufen Z (2004) Application of molecular absorption spectroscopy in the study of biomacromolecules. Spectrosc Spectral Anal 24(10):1197–1201

Cao AWG, Jiao B et al (2002) Study on the mechanism of color changes of commassie brilliant blue G-250. Acta Chim Sin 60(9):1656–1661

Cao WG, Zhao HQ, Jiao QC (2008) Mechanism of the interaction between coomassie brilliant blue and bovine serum albumin. Acta Laser Biol Sin 17(1):32–37

Chen Z, Liu G, Chen M, Peng Y, Wu M (2009) Determination of nanograms of proteins based on decreased resonance light scattering of zwitterionic gemini surfactant. Anal Biochem 384(2):337–342. https://doi.org/10.1016/j.ab.2008.10.006

Compton SJ, Jones CG (1985) Mechanism of dye response and interference in the Bradford protein assay. Anal Biochem 151(2):369–374. https://doi.org/10.1016/0003-2697(85)90190-3

Demchenko AP (1988) Site-selective excitation: a new dimension in protein and membrane spectroscopy. Trends Biochem Sci 3(10):374–377. https://doi.org/10.1016/0968-0004(88)90173-9

Duan A, Chen J, Liu H (2009) Application and development of molecular docking methods. J Anal Sci 25(4):473–477

Duhamel RC, Meezan E, Brendel K (1981) The addition of SDS to the Bradford dye-binding protein assay, a modification with increased sensitivity to collagen. J Biochem Biophys Meth 5(2):67–74. https://doi.org/10.1016/S0174-173X(83)80003-X

Falchi F, Caporuscio F, Recanatini M (2014) Structure-based design of small-molecule protein-protein interaction modulators: the story so far. Future Med Chem 6(3):343–357. https://doi.org/10.4155/fmc.13.204

Guo M, Jiang Y (1996) Effect of ingredients of coomassie brilliant blue color-developing reagent on protein assay. Prog Biochem Biophys 23(6):558–561

LãPez JM, Imperial S, Valderrama R et al (1993) An improved Bradford protein assay for collagen proteins. Clin Chim Acta 220(1):91–100. https://doi.org/10.1016/0009-8981(93)90009-S

Li R, Ren H, Sun Y et al (2006) Progress in analytical methodologies in non-covalent interactions between small-molecule and biomacromolecule. Chin J Anal Chem 34(12):1801–1806

Li R, Dai BC, Zhao YD et al (2009) Application and development of spectroscopy methodologies in the study on non-covalent interactions. Spectrosc Spectral Anal 29(1):240–243

Li GY, He Y et al (2012) Study on Interaction between Myricetin and Bovine Serum Albumin by Spectroscopy and Molecular Modeling. Acta Chim Sin 70(2):143–150. https://doi.org/10.6023/A1109211

Liang Y, Lin Q, Huang P, Wang Y, Li J, Zhang L, Cao J (2018) Rice bioactive peptide binding with TLR4 to overcome H_2O_2-induced injury in human umbilical vein endothelial cells through NF-kappa B signaling. J Agric Food Chem 66(2):440–448. https://doi.org/10.1021/acs.jafc.7b04036

Lloyd JBF (1971) Synchronized excitation of fluorescence emission spectra. Nat Phys Sci 231(20):64–65

Löffler BM, Kunze H (1989) Refinement of the Coomassie brilliant blue G assay for quantitative protein determination. Anal Biochem 177(1):100–102. https://doi.org/10.1016/0003-2697(89)90021-3

Macart M, Gerbaut L (1982) An improvement of the Coomassie Blue dye binding method allowing an equal sensitivity to various proteins: application to cerebrospinal fluid. Clin Chim Acta 122(1):93–101. https://doi.org/10.1016/0009-8981(82)90100-0

Morris GM, Lim-Wilby M (2008) Molecular docking. Methods Mol Biol 443(443):365–382. https://doi.org/10.1007/978-1-59745-177-2_19

Pinzi L, Rastelli G (2019) Molecular docking: shifting paradigms in drug discovery. Int J Mol Sci 20(18):4331. https://doi.org/10.3390/ijms20184331

Ren Y, Jiao X, Zhang L (2018) Expression level of fibroblast growth factor 5 (FGF5) in the peripheral blood of primary hypertension and its clinical significance. Saudi J Biol Sci 25(3):469–473. https://doi.org/10.1016/j.sjbs.2017.11.043

Ross PD, Subramanian S (1981) Thermodynamics of protein association reactions: forces contributing to stability. Biochemistry 20(11):3096–3102. https://doi.org/10.1021/bi00514a017

Schaffner W, Weissmann C (1973) A rapid, sensitive, and specific method for the determination of protein in dilute solution. Anal Biochem 56(2):502–514. https://doi.org/10.1016/0003-2697(73)90217-0

Shahabadi N, Maghsudi M, Kiani Z, Pourfoulad M (2011) Multispectroscopic Studies on the interaction of 2-tert-butylhydro-quinone (TNHQ), a food additive, with bovine serum albumin. Food Chem 124:1063–1068. https://doi.org/10.1016/j.foodchem.2010.07.079

Shin WH, Kihara D (2018) Virtual ligand screening using pl-patchsurfer2, a molecular surface-based protein-ligand docking method. Methods Mol Biol 1762:105. https://doi.org/10.1007/978-1-4939-7756-7_7

Spector T (1978) Refinement of the coomassie blue method of protein quantitation. A simple and linear spectrophotometric assay for less than or equal to 0.5 to 50 microgram of protein. Anal Biochem 86(1):142–146. https://doi.org/10.1016/0003-2697(78)90327-5

Sun L (2013) The study on protein variable temperature characteristics of Litopenaeus Vannamei based on Raman Specta technique. Jiangsu University, Zhenjiang

Wang YG, Jian-Zhong MA, Xue-Qing MA et al (2013) Optimization of brilliant blue g-250 dye solution using response surface methodology. Pharm Biotechnol 001:57–62

Wang L, Lin Q, Yang T, Liang Y, Nie Y, Luo Y, Shen J, Fu X, Tang Y, Luo F (2017) Oryzanol modifies high fat diet-induced obesity, liver gene expression profile, and inflammation response in mice. J Agric Food Chem 65(38):8374–8385. https://doi.org/10.1021/acs.jafc.7b03230

Ware WR (1962) Oxygen annihilation fluorescence in solution: experimental study of diffusion process. J Phys Chem 66(3):316–320. https://doi.org/10.1021/j100809a020

Wu D, Wang J, Liu D, Zang Y, Xia H (2019) Computational and spectroscopic analysis of interaction between food colorant citrus red 2 and human serum albumin. Sci Rep 9:1615. https://doi.org/10.1038/s41598-018-38240-9

Yang M, Abdalrahman H, Sonia U, Mohammed A, Vestine U, Wang M, Ebadi AG, Toughani M (2020) The application of DNA molecular markers in the study of Codonopsis species genetic variation, a review. Cell Mol Biol 2:23–30. https://doi.org/10.14715/cmb/2020.66.2.3

Zhang G, Ma Y, Wang L et al (2012) Multispectroscopic studies on the interaction of maltol, a food additive, with bovine serum albumin. Food Chem 133:264–270. https://doi.org/10.1016/j.foodchem.2012.01.014